



Relationship between container ship underwater noise levels and ship design, operational and oceanographic conditions

Megan F. McKenna, Sean M. Wiggins & John A. Hildebrand

University of California San Diego, Scripps Institution of Oceanography 8635 Kennel Way La Jolla, CA 92093-0205.

SUBJECT AREAS:
PHYSICAL SCIENCES
ENVIRONMENTAL SCIENCES
ECOLOGY
APPLIED PHYSICS

Received
13 November 2012

Accepted
9 April 2013

Published
2 May 2013

Correspondence and requests for materials should be addressed to M.F.M. (megan.mckenna@gmail.com)

Low-frequency ocean ambient noise is dominated by noise from commercial ships, yet understanding how individual ships contribute deserves further investigation. This study develops and evaluates statistical models of container ship noise in relation to design characteristics, operational conditions, and oceanographic settings. Five-hundred ship passages and nineteen covariates were used to build generalized additive models. Opportunistic acoustic measurements of ships transiting offshore California were collected using seafloor acoustic recorders. A 5–10 dB range in broadband source level was found for ships depending on the transit conditions. For a ship recorded multiple times traveling at different speeds, cumulative noise was lowest at 8 knots, 65% reduction in operational speed. Models with highest predictive power, in order of selection, included ship speed, size, and time of year. Uncertainty in source depth and propagation affected model fit. These results provide insight on the conditions that produce higher levels of underwater noise from container ships.

Maritime shipping constitutes a major source of low-frequency noise in the ocean^{1–3}, particularly in the Northern Hemisphere where the majority of ship traffic occurs. At frequencies below 300 Hz, ambient noise levels are elevated by 15–20 dB when exposed to distant shipping^{4–6}. Underwater ship noise is an incidental by-product from standard ship operations, mainly from propeller cavitation⁷. Concerns have been raised over the effects of these increased noise levels on marine life^{8–11}. Yet, predicting noise levels from ships in a given region and the specific conditions that may increase these levels remains largely unexplored.

The Santa Barbara Channel (SBC), off the coast of southern California (Fig. 1), is a region of intense commercial vessel traffic, concentrated in designated shipping lanes with an average of eighteen ships transiting per day¹². Two major ports, Port Hueneme and Port of Los Angeles-Long Beach (POLA), serve ships traveling through the SBC. POLA is the second busiest port in North America and until recently, an estimated 75% of vessel traffic departing from and 65% of traffic arriving at POLA and Port Hueneme traveled through the SBC¹².

Container ships, the focus of this study, are a specific class of large commercial vessels designed to hold containerized cargo (Fig. 2) and represent a highly efficient transport system. These ships are big and fast with comparatively short port time and transport almost 90% of general cargo¹³. Regionally, container ships represent the majority of the commercial vessels¹²; globally, they represent 22% of the commercial fleet¹³. Container ships were introduced in the 1950s, and since 1990 container trade has seen a five-fold increase; the fastest growth of any ship-type. In this study, we collected seafloor acoustic measurements of transiting container ships in the SBC to determine what variables (design, operational, and oceanographic) relate to the measured levels of underwater noise.

Ship design characteristics (e.g. length, gross tonnage), operational condition (e.g. speed), and the oceanographic setting (e.g. month, wave height) collected during each individual ship passage were used as covariates to develop a statistical model to relate the level of underwater noise from ships to these variables. Statistical models were built for broad-band source level estimates (20–1000 Hz) and five low-frequency octave bands using nineteen covariates to determine if measured predictors explain the noise levels, the relationships are significant, and ascertain the contributions of different variables. Sound levels from multiple transits of the same ships were also evaluated. The results of this study provide details on ship characteristics and sea conditions that

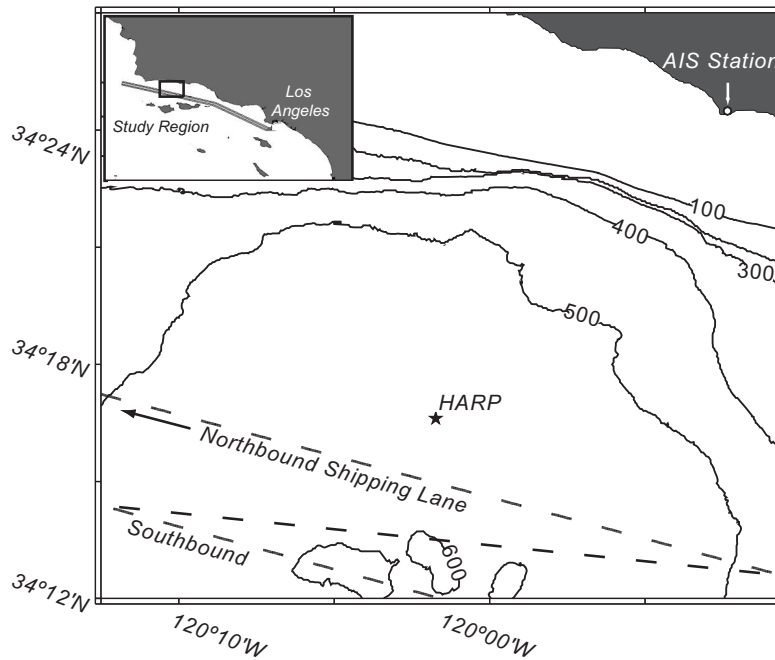


Figure 1 | Map of SBC, a region off the coast of southern California (inset). The location of the HARP ($34^{\circ}16.617'N$ and $120^{\circ}01.492'W$), AIS receiving station ($34^{\circ}24.5'N$ and $119^{\circ}52.7'W$), north and southbound shipping lanes (dashed lines), and 100 m bottom contours are shown. The map was created using Matlab- Mapping Toolbox.

result in higher levels of underwater noise for a relatively new ship-type with continuing growth in global activity¹³.

Results

Source levels (SL) for 593 container ship transits were estimated from long-term acoustic recording received levels (RL) and a simple transmission loss model using Automatic Identification System (AIS) data for source-receiver range. Forty-five percent of the measured ships made two or more transits and 5% had four or more transits (Fig. 3). Using a suite of operational and oceanographic covariates (Table 1) to predict the SL of these 29 ships, individual ship identification was not selected as a covariate and therefore, did not improve explained deviance in the Generalized Additive Models (GAM) results for any of the modeled frequency bands. There was a slight increasing trend of larger ships having higher broad-band SL; however SL for an individual ship, in some cases, varied by 5–10 dB (Fig. 3). Based on these results, each ship transit was considered an independent event and ship identification was not included as a covariate in the preceding models.

All statistical models significantly improved in explained deviance with the addition of operational and oceanographic covariates. Specifically, the explained deviance using the best-fit model with only design predictors was never greater than 25%. When operating and oceanographic covariates were included, explained variability in SL



Figure 2 | Photograph of container ship transiting the SBC (credit J. Calambokidis, Cascadia Research).

increased to greater than 39%. Deviance explained was highest for the broad-band best-fit model (56%) and in general fit decreased with increasing frequency band (Table 2).

In all frequency band models, the operational variable, ship speed (SPD), was included as a covariate and explained the most variability in SL (Table 2; Fig. 4). The additional design, operational, and oceanographic covariates and relative importance in the models varied depending on frequency band. The number of covariates included in the best-fit models ranged from 4 to 8; the lower frequency band models included more covariates and in general had higher explained deviance in SL.

A measure of ship size (length over all (LOA) or gross tonnage (GT)) was selected as a covariate in predicting SL in all frequency bands (Table 2). Ship length, LOA, was the important design covariate for lower frequency bands, while, GT was the important design covariate for higher frequency bands. For the 124 and 250 Hz models, when ships were shorter than expected based on GT, SL predictions were higher. For the 63 Hz band, when ships had greater horsepower (HP) than expected based on GT, higher SL was predicted. Inclusion of oceanographic covariates varied depending on frequency band model (Table 2). Month (MTH) of the measurement was included as a covariate in all frequency band models; the best-fit models predicted higher SL in the spring. For the lower frequency models (16 and 31.5 Hz) and the broad-band model, wave height and current direction were included as predictors of SL. As wave height increased and when the sea surface current was opposite the direction the ship was traveling, higher SL was predicted. For the higher frequency best-fit models, covariates for ocean surface conditions were not included as covariates.

In some of the frequency band models, range to the seafloor recorder (RAN) and distance to another ship (OTH) were selected as covariates in the best-fit models (Table 2). For example, in the 124 Hz model, ships at closer ranges to the HARP had higher predicted SL. For octave-bands centered at 250 and 500 Hz and the broad-band model, the presence of tones resulted in higher predicted source levels. Narrowband tones were present in 10% of the measured ships (Fig. 5).



Predictor Variable	Abbreviation	Description
<i>Ship Design</i>		
Length	LOA	total length of ship in meters
Gross tonnage	GT	unit less index related to ships overall internal volume
Horsepower	HP	measurement of engine power
Service speed	SSPD	speed the ship was designed to travel at for maximum efficiency
Draft	DFT	average vertical distance between the waterline and the bottom of the hull
Identification year built	ID YB	Maritime Mobile Service Identity (MMSI), a series of 9 digits to uniquely identify ships year the ship was constructed
<i>Operational</i>		
Speed	SPD	actual ship speed over ground
Range	RAN	distance of the ship to the HARP at closest point of approach
Proportion of speed	PSPD	proportion of the service speed the ships is travelling (SPD/SSPD)
Other ship	OTH	time to the next ship passage (> 1 hour)
Tones	TONE	presence of spectral tones
<i>Oceanographic</i>		
Month	MTH	month of the year
Wave height	WVHT	significant wave height (meters) is calculated as the average of the highest one-third of all of the wave heights during the 20-minute sampling period
Wave direction	MWD	mean wave direction corresponding to energy of the dominant period (DPD). The units are degrees from true North
Current direction	CDIR	direction the ocean current is flowing toward. 0–360 degrees, 360 is due north, 0 means no measurable current
Wave period	DPD	dominant wave period (seconds) is the period with the maximum wave energy
Wind direction	WDIR	wind direction measurements in degrees clockwise from true North
Wind speed	WSPD	wind speed values in m/s

Discussion

The results of this study reveal how low-frequency noise from commercial maritime vessels relates to a suite of covariates describing the vessel passages. The statistical approach of this study provided a framework to evaluate possible covariates for predicting underwater noise. Covariates differed depending on the frequency band analyzed; however, all models included speed and a measure of ship size, corroborating earlier studies that predicted higher noise levels from faster and larger ships^{7,14,15}. Our

results expand on these previous findings by measuring noise from a modern ship-type, the container ship, measuring over a broader frequency range, and including additional covariates that describe the oceanographic setting. Although we found substantial variation, even on a ship by ship comparison, considerations of these predictors are important when quantifying the level of ship noise in a particular region. The opportunistic approach of this study can be used to evaluate specific changes in design and measure other ship-types.

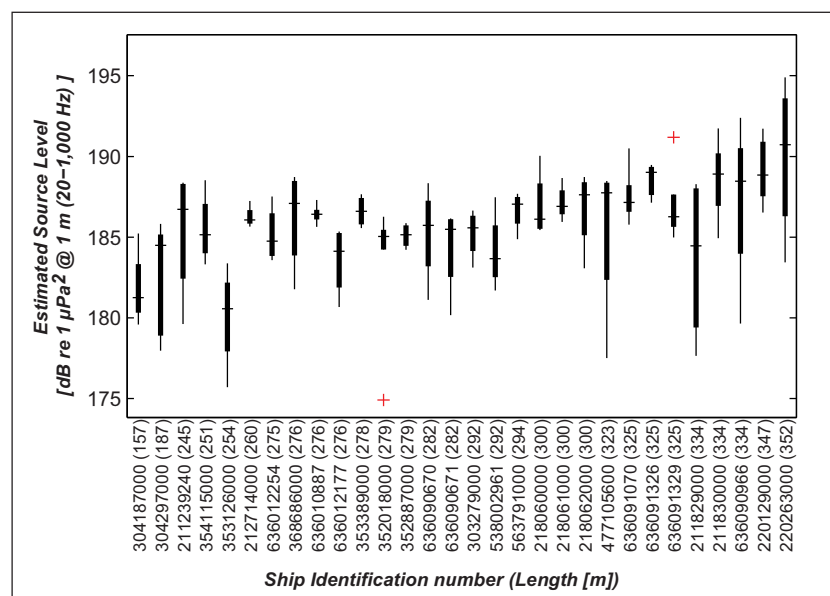


Figure 3 | Variability individual container ship estimated SL from ships that transited on four or more different occasions. Boxes bound the 25th and 75th percentiles with the horizontal line at the median. Ends of the vertical whiskers are the highest and lowest values of the data set that are within 1.5 times the inter-quartile range of the box edges. The plus signs represent data outside the range of the whiskers.



Table 2 | Summary of GAM results for each frequency band. * indicates values for evaluating best-fit model for a given frequency band; ** indicates values used to compare between different best-fit models

EQUATION- with covariates in the order of importance	AIC*	Residual deviance*	% of deviance explained**	No. covariates**
BROAD-BAND (20–1,000 Hz)				
BB ~ SPD + LOA + MTH + s(rSSPD,3) + TONE + MWD + s(WVHT,2) + CDIR	2834.5	3826.3	56	8
OCTAVE BAND CENTERED AT 16 Hz				
OB16 ~ SPD + LOA + MTH + WVHT + s(RAN,3) + rSPD + MWD + CDIR	3341.9	9003.2	54	8
OCTAVE BAND CENTERED AT 31.5 Hz				
OB31 ~ SPD + LOA + MTH + WVHT + YB + s(CDIR,2) + s(OTH,3) + rSPD	3294.3	8252.7	53	8
OCTAVE BAND CENTERED AT 63 Hz				
OB63 ~ s(SPD,2) + rHP + s(RAN,3) + MTH + s(GT,3) + s(OTH,3)	3109.4	6021.7	43	6
OCTAVE BAND CENTERED AT 124 Hz				
OB125 ~ SPD + MTH + s(GT,3) + s(RAN,2) + rLOA	2992.9	5083.2	38	5
OCTAVE BAND CENTERED AT 250 Hz				
OB250 ~ SPD + MTH + GT + TONE + s(rSSPD,3) + rLOA + s(RAN,2)	3022.0	5284.7	44	7
OCTAVE BAND CENTERED AT 500 Hz				
OB500 ~ s(SPD,2) + MTH + TONE + GT	3192.9	7146.0	39	4

The rapid increase in world shipping, along with the increase in ship speed and size, has been correlated with increases in low-frequency ambient noise in the Northeast Pacific⁵. This study supports this relationship: models in all frequency bands predicted higher SL with increased ship speed and size. Furthermore, ship speed explained most of the variability in container ship SL in all frequency bands, and a metric of ship size was included in all models. Ross (1976) reported a similar positive relationship between overall source spectral level above 100 Hz and speed and size of the vessel for ships < 30 kGT, smaller than the ships analyzed in this study. More recent studies relating ship noise to speed did not find evidence for a positive relationship between speed and SL^{15,16}. The lack of a relationship may be an artifact of combining multiple ship-types into a single regression analysis⁶. Specific ship-types have unique designs

(e.g. hull shape, machinery) directly influencing the spectral characteristics of underwater radiated noise⁶. This study controlled for ship specific differences by performing statistical analyses on only one ship-type, the container ship, to understand predictors of container ship noise levels.

Although a measure of ship size was included as a covariate in predicting SL in all frequency bands, the size variable differed. Ship length was the important design covariate for lower frequency bands, while, *GT* was the important design covariate for higher frequency bands. Our results also indicated that for ships shorter than expected based on *GT* had higher predicted source level; these ships are likely post-panamax ships, a design change that allowed for increases in breadth but no change in length. The parameters used in our models were general descriptions of ship design, inclusion of more specific

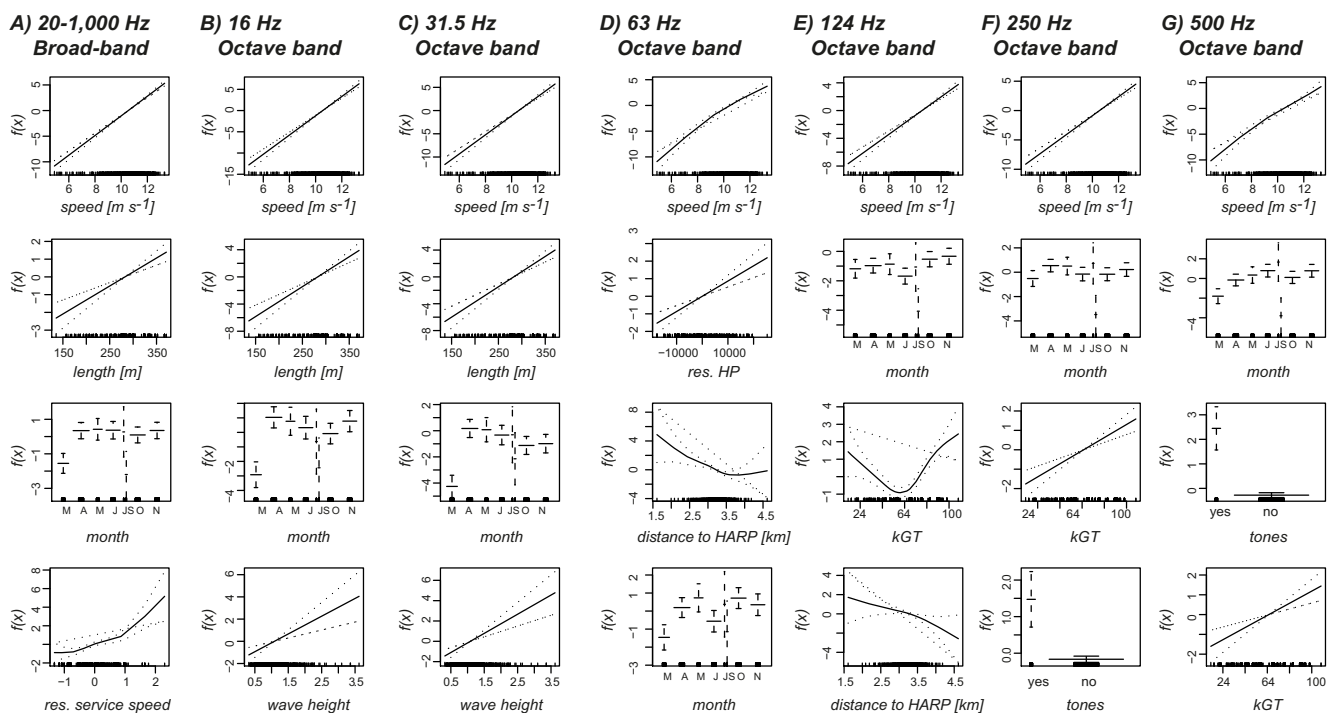


Figure 4 | Generalized additive model functions for ship SL. For each frequency band model (A-G), functions shown are for the four variables with the most predictive power (Table 3). The rows are ordered according to predictive power (*i.e.*, the first row are the predictors that had the highest predictive power in the step-wise model selection procedure). Functions are scaled relative to the model mean (note different y-axis scales). *MTH* and *TONE* were modeled as categorical variables; the width of each bar represents the sample size and dashed lines are two standard error bands.

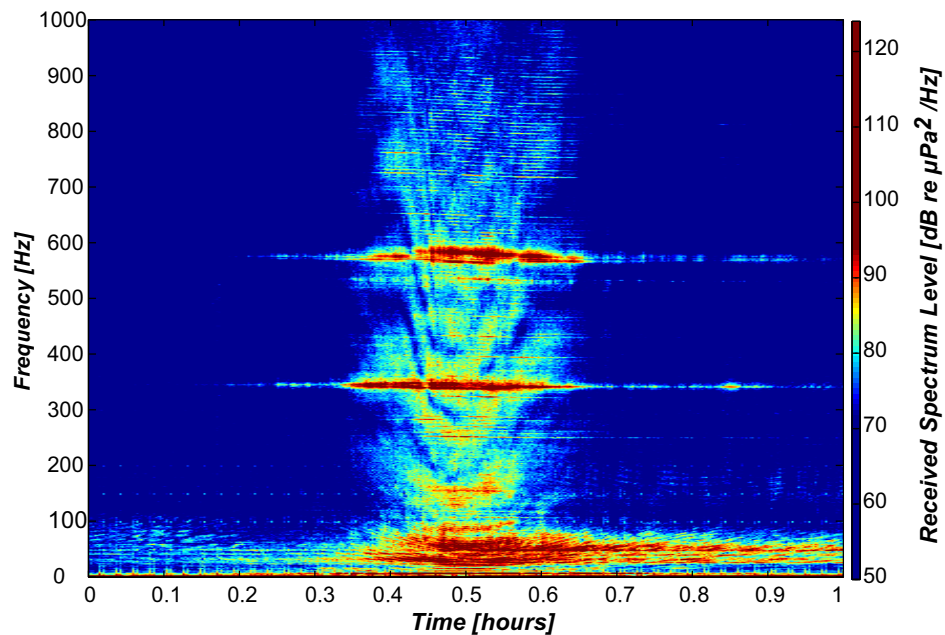


Figure 5 | Spectrogram of received sound spectrum levels during a 1-hour passage of a container ship. The spectrogram is centered on the CPA of the ship to the HARP, a distance of 3 km. The intense tones present at approximately 350 and 580 Hz are representative of the tones present in 10% of the container ships in this study.

descriptors of propeller and hull design (e.g. block coefficient, resistance, propeller shape) although not part of AIS data stream would likely improve model results and allow for more specific design recommendations.

In addition to ship speed and size, oceanographic variables describing the ocean surface conditions during each ship's transit were included as covariates in the statistical models. Of the seven possible oceanographic variables, month (*MTH*) of the ship passage

was included as a covariate in all models. This predictor was intended to capture differences in radiated noise related to water column properties, specifically sound speed profiles (SSP) which are influenced by seasonal water temperatures that change the propagation characteristics. Given the opportunistic approach of this study, obtaining simultaneous SSP, although ideal for determining propagation loss, was not possible. All statistical models tended to show an increase in predicted radiated noise during the spring months

Table 3 | Comparison of delta AIC values from the step-wise GAM procedure for the best-fit model in each frequency band (blank boxes indicate that the covariate was not included in the best-fit model). AIC values are compared to the null model and greatest delta AIC values indicate the most improvement from the null model

Variable		delta AIC						
<i>Ship Design</i>		<i>Broad-band</i>	16 Hz	31.5 Hz	63 Hz	124 Hz	250 Hz	500 Hz
Length	<i>LOA</i>	30.6	40.7	52.8		6.1	3.1	
Gross tonnage	<i>GT</i>				12.5	50.0	16.5	11.9
Horsepower	<i>HP</i>				24.9			
Service speed	<i>SSPD</i>	32.9					39.1	
Draft	<i>DFT</i>							
Identification	<i>ID</i>							
Year built	<i>YB</i>			13.6				
<i>Ship Operational</i>		<i>Broad band</i>	16 Hz	31.5 Hz	63 Hz	124 Hz	250 Hz	500 Hz
Speed	<i>SPD</i>	323.7	291.9	257.9	203.4	173.2	206.8	181.4
Range	<i>RAN</i>		10.5		17.2	6.4	2.3	
Proportion of speed	<i>PSPD</i>		9.2	1.9				
Other ship	<i>OTH</i>			2.6	4.9			
Tones	<i>TONE</i>	11.8					10.0	30.6
<i>Environmental</i>		<i>Broad band</i>	16 Hz	31.5 Hz	63 Hz	124 Hz	250 Hz	500 Hz
Month	<i>MTH</i>	25.9	37.8	46.5	11.0	12.2	18.8	36.9
Wave height	<i>WVHT</i>	4.8	15.5	13.4				
Wave direction	<i>MWD</i>	4.8	3.9					
Current direction	<i>CDIR</i>	3.8	3.0	4.7				
Wave period	<i>DPD</i>							
Wind direction	<i>WDIR</i>							
Wind speed	<i>WSPD</i>							



(April, May and June). Spring water column properties in this region provide a possible explanation for this result. During the spring, strong upwelling events occur in this region, introducing cold water to the surface resulting in a more uniform water column¹⁷. During the late summer and fall, warmer surface waters trap sound waves when the sound source is within the warm surface layer, resulting in less radiated noise¹⁸. Further supporting this explanation is the greater importance of *MTH* as a covariate in the higher frequency models; as the trapping of sound in the surface layer has a greater effect in the higher frequencies¹⁸. Unfortunately, not all months are represented in this study, somewhat limiting the seasonal comparisons. Furthermore, ephemeral coastal oceanographic features such as internal waves could also influence sound propagation in surface waters on shorter time scales¹⁹.

Surface current direction was another important predictor of ship noise in the lower frequency models. When the surface current was

opposite to a ship's direction of travel, predicted noise levels were higher. This was expected given that for a ship to achieve its optimal operational speed an increase in engine power is needed, potentially increasing radiated noise. In the lower frequency bands, the wave height, dominant wave period, and direction of the dominant wave period also influenced predicted noise levels. Increased wave height and decreased wave period create rougher seas, causing ships to roll and pitch, likely resulting in increased cavitation and the predicted radiated noise levels. Weather conditions are known to influence the ambient noise levels at frequencies measured in this study, although at much lower levels than from ships¹³; and in the model selection process, wind speed and direction were not included as covariates in any of the models of radiated ship noise.

For some frequency bands (16, 63, 124, and 250 Hz), an increase in SL level was predicted for ships transiting closer to the HARP. Specific ship behaviors might explain why levels were higher when

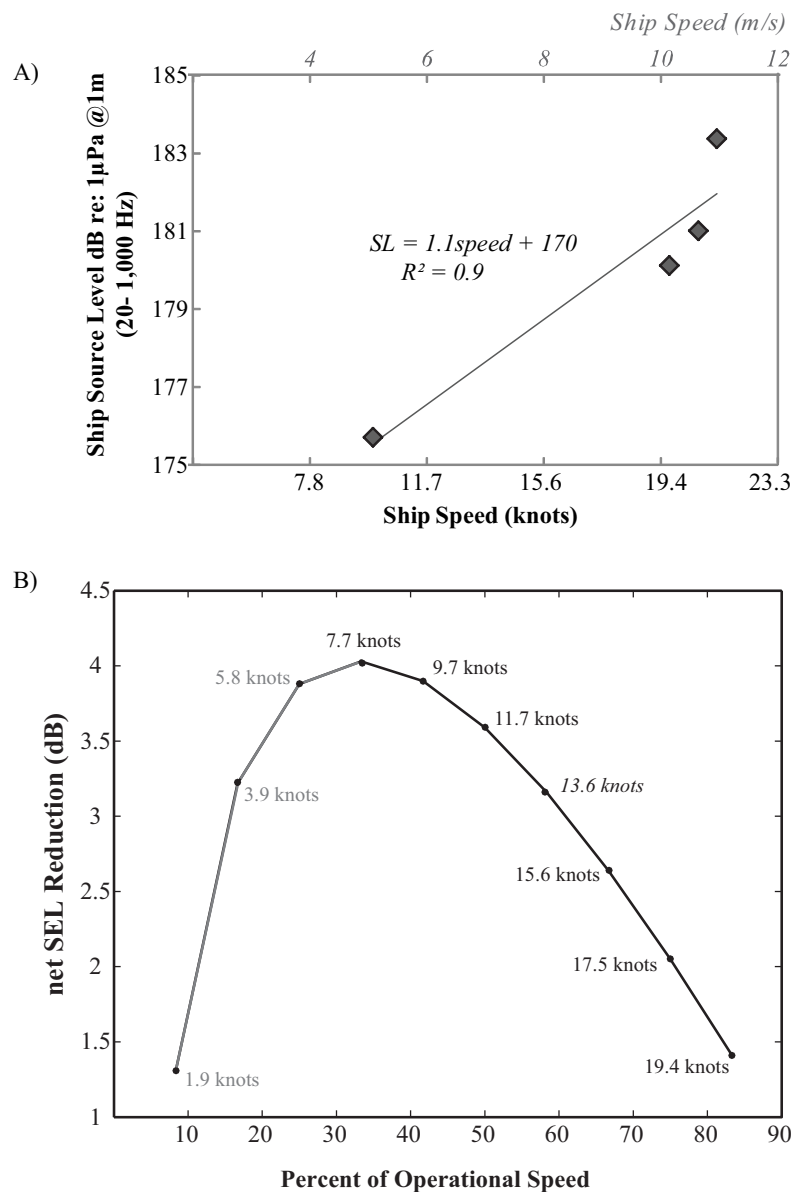


Figure 6 | (A) Relationship between broad-band SL and speed for a 294 m container ship that transited the region on four separate days (10/17/2008, 11/21/2008, 04/10/2009, and 05/14 2009). Equation for the linear relationship and goodness of fit value (R^2) are shown. (B) The net reduction in SEL for the container ship in (A) for different speeds. The derived curve is based on the relationship between SL and speed (A) and known operation speed of 12 m/s (23.3 knots). The gray part of the curve indicates that these speeds are likely not possible for a container ship.

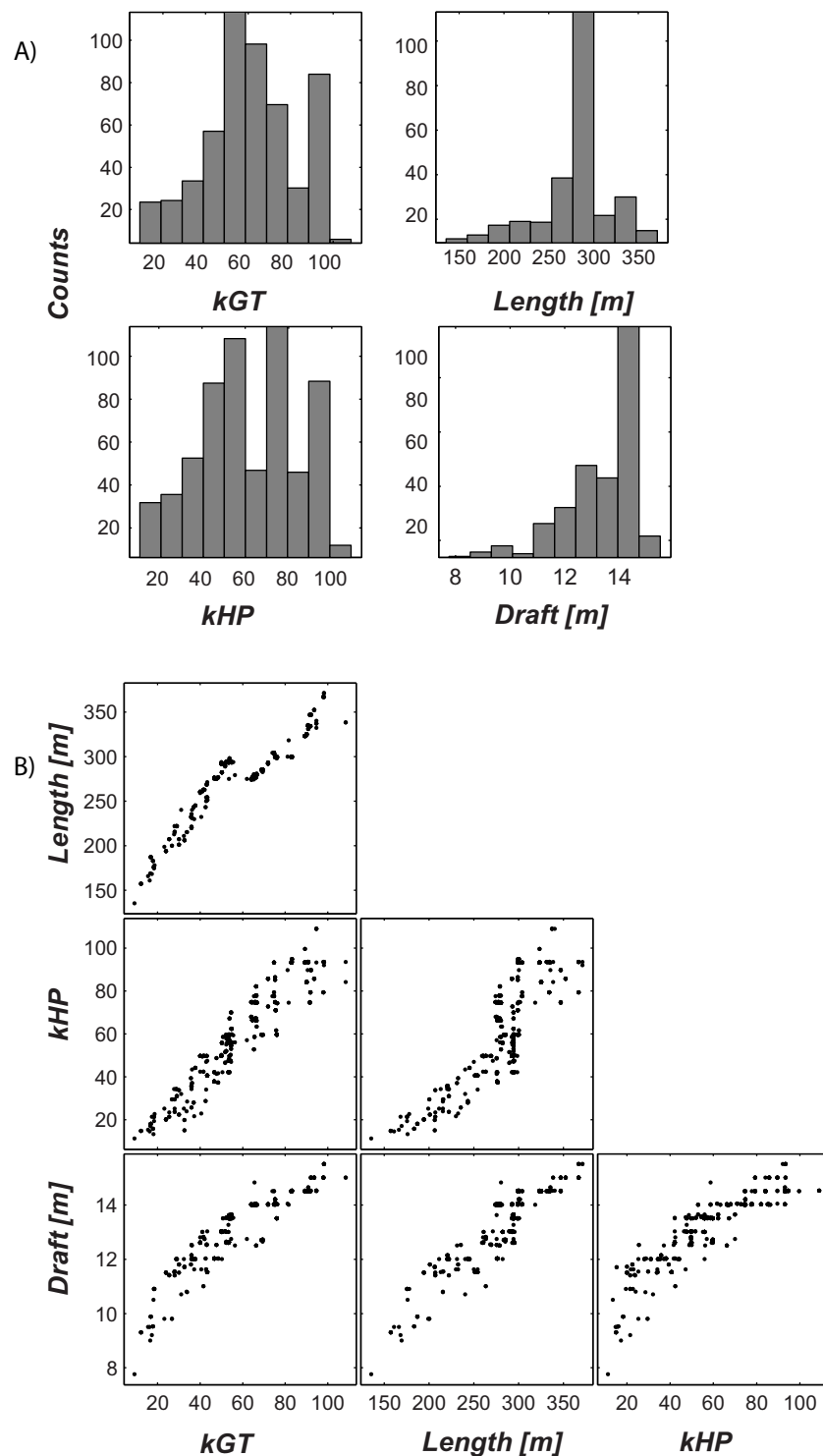


Figure 7 | Comparison of container ship design characteristics. (A) Distributions of design variables (B) Correlations of different design characteristics, including gross tonnage (kGT), ship length, horse power (kHP) and drafts are shown for 593 container ships.

ships were closer to the HARP. A spatial analysis of ship speed in the region showed that faster ships travel on the outside of the lanes (*i.e.*, closer to the HARP)²⁰. Based on this observation, this variable likely relates to ship speed; however, it might also relate to how sound propagates and interacts with the seafloor at different distances to the receiver. We limited our analysis to individual ships transiting the SBC without other ships (>1hour between passages), but included time between the passing ships as a possible covariate in the models.

Only lower frequency bands (31.5 and 63 Hz octave-bands) included this duration as a covariate and inclusion might relate to the propagation of low frequency sound from distant ships.

Multiple recordings of individual ships on different transits provided a comparison of SL from the same ship (Fig. 3). The 5–10 dB variability suggested that either operational conditions and/or the oceanographic settings had a significant influence on the radiated noise. This result, although important for understanding conditions



that might lead to higher noise levels from ships, presents a challenge for targeting individual ships to reduce overall noise from the noisiest ships. One important covariate, the presence of spectral tones, might result in significant reductions in noise. Ships with tones had higher predicted noise levels in both the broad-band and high frequency octave bands (250 and 500 Hz). The cause of these tones is unknown, but may relate to propeller damage which may increase radiated noise, and potentially decrease efficiency of the propulsion system⁷. Identifying these ships and eliminating the cause of the tones would result in a significant reduction in noise.

The age of a ship was a covariate in the 31.5 Hz octave band model: older ships produced more noise in this band. Most of the ships analyzed in this study were built between 2000 and 2005 (47%), 19% were built after 2005, and the remaining ships were built prior to 2000; the oldest container ship included was built in 1971. Changes to the propulsion system in newer ship builds might explain the decreased amount of low-frequency radiated noise, even though newer ships travel at faster speed and are, on average, larger. Container ship design has seen continued improvements both in the reduction of ship resistance through the water and increased propulsion and machinery efficiency²¹. Improvements include dampening of engine vibrations, changes in hull design, and a reduction in the number of engine cylinders²¹. Propeller damage or fouling on older ships might also explain the higher levels of radiated noise predicted for older ships.

Given that ship speed was the most important covariate in predicting SL, ship speed reduction should result in lower radiated sound levels. However, ship SL is an instantaneous estimate of radiated noise and strategies to reduce noise from shipping must consider the cumulative noise exposure, especially when slowing ships in a particular region. One method to calculate cumulative

exposure is Sound Exposure Level (SEL) or the integration of the noise over a specific duration:

$$SEL = SL + (10 \times \log_{10}(\text{time}[s]))$$

There is a trade-off between traveling slower (decrease in SL) and spending more time in an area (increase time) for the SEL calculation. For example, a 294 m container ship was recorded traveling at 10 m/s and 5 m/s (Fig. 6A). The SL for this ship was 5 dB less for the slower passage, but the time spent in the area increased two-fold resulting in a 3 dB increase in noise; therefore, the net reduction in SEL was only 2 dB for the slower ship. To calculate the net reduction in SEL for any speed the following equation was derived using the relationship between speed and SL (Fig. 6A) and the ship's operational speed (service speed):

$$\text{net SEL reduction}(dB)_i = (SL_o - (1.1spd_i + 170)) - 10 \times \log_{10} \frac{spd_i}{spd_o}$$

where, i is a specific speed iteration, spd_o is the known operational speed of the ships, and SL_o is the estimated ship source level at operational speed. In this example, the spd_o was 12 m/s and SL was 183.2 dB re: 1 μ Pa @ 1 m. The maximum net reduction in SEL occurred when the ship traveled at 4 m/s (7.7 knots) or 35% of operational speed (Fig. 6B). Noise reduction efforts could focus on ships with tones, older ships, and reducing vessel speeds. However, vessel speed reduction should consider cumulative noise, specifically the trade-off between SL reduction and time spend in a region and the feasibility of a ship traveling at speeds slower than their operational speed.

Variability in SL that remained unexplained by our statistical models may be related to the depth of the propeller, the main sound source. A shallower source depth will decrease the effect of the dipole

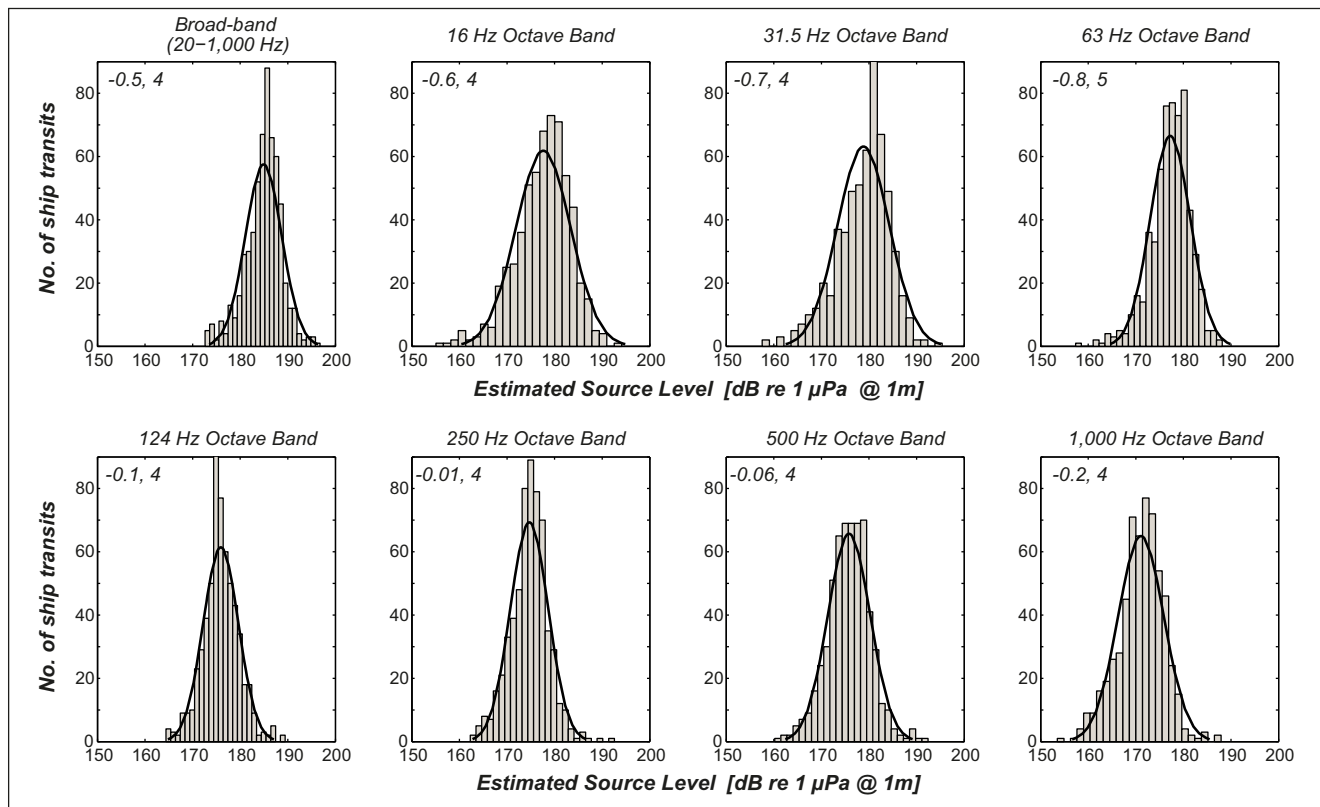


Figure 8 | Distribution of estimated container ship SL by frequency band. The number of bins equals the square root of the number of ship transits, with a fitted normal distribution. The skewness (measure of asymmetry of the data around the mean, negative indicated left skew) and kurtosis (measure of outliers, where 3 is considered normal) are shown in the upper left corners.



source; thereby decreasing the amount of radiated sound from the ship. In other words, the closer the source is to the sea surface the lesser the strength of the dipole⁷. Source depth will vary depending on the particular design of a ship and the load conditions during a specific transit. Unfortunately, AIS does not provide information on the load conditions of the ship; therefore, it was not possible to include this covariate in the models. The models included the ship's specified optimal draft. This variable, however, was not selected as a covariate in any of the models, suggesting that ship draft was not a good proxy for the actual depth of the source. Perhaps other metrics, such as the number of loaded containers, might be more accurate prediction of propeller depth. In general, container ships leaving POLA (*i.e.*, northbound) are not as loaded as when they enter²². Measurements reported in this study are from ships departing POLA (northbound), potentially over representing ships that are not fully loaded and underestimating the radiated noise from fully loaded ships, likely with a deeper source.

Methods

Acoustic recordings. High-frequency acoustic recording packages (HARPs) were deployed in the SBC, approximately 3 km from the northbound shipping lane (Fig. 1). HARPs are bottom-mounted instruments containing a hydrophone, data logger, battery power supply, ballast weights, acoustic release system, and flotation²³. The hydrophone is tethered to the instrument and buoyed approximately 10 m above the seafloor. All acoustic data were converted to absolute sound spectrum levels using Fast-Fourier Transforms (2000 Hz sampling rate, 2000 samples, 0% overlap, Hanning window) and based on hydrophone calibrations performed at Scripps Institution of Oceanography Whale Acoustics Laboratory and at the U.S. Navy's Transducer Evaluation Center facility in San Diego, California. The amount of time used in the sound spectrum level calculation was equal to the time it took the ship to travel its own length, as suggested by Bahtiaran (2009) and detailed in the Acoustical Society of America (ASA) standard (ANSI/ASA S12.64-2009/Part 1).

Opportunistic acoustic recordings of passing ships were collected October–November 2008 and March–October 2009, excluding August. Long-term acoustic recordings were combined with ship passage information from AIS²⁴ to estimate ship source level using the same methods described in McKenna *et al.* (2012)⁶. Received sound levels were measured at the closest point of approach (CPA) of each ship transiting the northbound shipping lane to the HARP (Fig. 1). CPA distances ranged from 1.6 to 4.6 km. Total broad-band noise level (20–1000 Hz) and noise levels in standard octave bands, centered at 16, 31.5, 63, 124, and 500 Hz were calculated by summing the mean squared pressure values in each 1-Hz frequency bin, and converted back to sound pressure levels expressed as decibels referenced to a unit sound pressure density in sea water (1 μ Pa). To estimate SL for each transiting ship, approximated sound transmission loss (TL) at the CPA distance (typically \sim 3 km) was added to the measured ship RL at CPA. A spherical spreading transmission loss model was used (*i.e.*, $TL = 20 \cdot \log_{10}(\text{Range}[m])$; see McKenna *et al.*, 2012⁶ for justification). By using a long duration measurement and broad frequency band, interference patterns resulting from the dipole source near the surface and bottom reflection were averaged out, providing an estimate of SL. All acoustic data matching the CPA times were evaluated for the presence of a single ship and eliminated if another ship passed within 1-hour or if vocalizing marine mammals were present.

Ship operational variables. The AIS data provided information on the operating conditions of each ship transit. Four variables were collected and used as covariates in the statistical models: speed *SPD*, range to the receiver *RAN*, time to the next ship passage *OTH*, and the proportion of the service speed the ship was traveling at *PSPD* (Table 1). The speeds reported by AIS, are speeds over ground, not actual speed of the ship relative to surface currents. The AIS speeds were adjusted to actual speed based on the surface current speed and direction. Archived surface current data were obtained from the University of California Santa Barbara, surface current mapping project²⁵. One additional operational variable gathered from the acoustic data was the presence of narrow-band frequency tones *TONE*. This was a simple binomial variable, present or absent.

Ship design variables. Only ships classified as container ships greater than 100 m in length were included in this analysis. For these ships, seven additional ship design variables were gathered from the World Shipping Encyclopedia²⁶ by matching the unique ship identification from AIS with this database. The seven variables collected were ship identification *ID*, gross tonnage *GT*, service speed *SSPD*, length overall *LOA*, draft *DFT*, horse power *HP*, and year built *YB* (Table 1). Many of the ship design variables are highly correlated (Fig. 7) and to avoid ambiguous model results, the residuals from linear fits between variables were used as covariates in the models.

Oceanographic variables. Sea conditions during each ship passage were obtained from archived data at the National Oceanic and Atmospheric Administration, station 46053 (32°14.9'N 119°50.5'W)²⁷. The six oceanographic conditions measured during the same hour as the passage of each ship included: ocean surface current direction

CDIR, wind direction *WDIR*, wind speed *WSPD*, significant wave height *WVHT*, dominant wave period *DPD*, and dominant period wave direction *MWD* (Table 1). The month of the acoustic measurement *MTH* was also included as a general representation of water column properties.

Statistical approach. For each frequency band, generalized additive models (GAM)²⁸ were used to relate ship source level to the ship characteristics described above. GAMs are well suited for modeling distribution data since the constraint of linearity is lifted and a more flexible approach to the relationship between covariates can be taken. We fit GAMs using the *step.gam* software package (*R Project for Statistical Computing* 2.12.2). The shapes of the distributions of source levels in each frequency band were used to choose identity link functions (Fig. 8). Each predictor variable was evaluated with and without smoothing splines where the number of knots for smoothed functions was constrained to either 2 or 3²⁹. The best-fit model was selected using Akaike's Information Criterion (AIC):

$$AIC = -2 \cdot \ln(L(\Theta|y)) + 2 \cdot P$$

where, $L(\Theta|y)$ is the likelihood of the parameters given the data y , and P is the number of parameters. The best-fit model minimizes AIC by maximizing the log-likelihood, with penalties for the number of parameters included³⁰. For purposes of evaluating covariates in the models, we used a step-wise approach and present the delta AIC value for each covariate relative to the null model AIC value (Table 3). AIC is a powerful model selection technique, but only compares models during the selection process, and does not give any indications of the significance of a particular model fit to the data or allow for comparisons between different models (in this case the frequency band models). Therefore, the best-fit model for each frequency band was also verified using an analysis of explained deviance, comparing the residual deviance of several models using a chi-square method. The best-fit model was one that minimized both AIC and residual deviance. Each model result is summarized by AIC values, percent explained deviance, and expressed as an equation:

$$SL_{\text{Eq band}} \sim \text{predictor 1} + s(\text{predictor 2, } x) + s(\text{predictor 3, } y) + \dots$$

where, $SL_{\text{Eq band}}$ is the response variable the model is predicting, *predictor 1* represents a linear covariate, $s()$ represents a smoothing function for a given predictor, x represents the number of knots (*i.e.*, smoothing constraints), and y represents the number of knots in a subsequent smoothing function.

All model trials were run separately for each frequency band (e.g. broad-band and four octave bands). Using the GAM approach, we first modeled a subset of ships, specifically individual ships that had four or more transits, to determine if specific ship (as a categorical variable and random effect in a generalized linear model) improved model fit. If not, each ship transit was considered an independent event. Only operational and oceanographic covariates were included in these trials given that the design variables did not change for individual ships. A second set of GAMs were used to determine what design variable described the most variability in estimated SL; using the step-wise approach delta AIC values were used to determine the covariate that explained the most variability. The resulting design variable was then used to transform the other ship design variables into residuals of the main design variable (*rGT*, *rSSPD*, *rLOA*, *rDFT*, *rHP*, *rYB*). After the correlated designed variables were transformed, a third set of GAMs were run with all predictor variables (Table 1) to relate ship SLs to the covariates.

- Hildebrand, J. A. Anthropogenic and natural sources of ambient noise in the ocean. *MEPS* **395**, 5–20 (2009).
- Wagstaff, R. A. Low-frequency ambient noise in the deep sound channel- The missing component. *J. Acoust. Soc. Am.* **69**, 1009–1014 (1981).
- Wenz, G. Acoustic ambient noise in the ocean: spectra and sources. *J. Acoust. Soc. Am.* **34**, 1936–1956 (1962).
- Andrew, R., Howe, B., Mercer, J. & Dzieciuch, M. Ocean ambient sound: Comparing the 1960's with the 1990's for a receiver off the California coast. *Acoustic Research Letters Online* **3**, 65–70 (2002).
- McDonald, M. A., Hildebrand, J. A. & Wiggins, S. M. Increases in deep ocean ambient noise in the Northeast Pacific west of San Nicholas Island, California. *J. Acoust. Soc. Am.* **120**, 711–718 (2006).
- McKenna, M. F., Ross, D., Wiggins, S. M. & Hildebrand, J. A. Underwater radiated noise from modern commercial ships. *J. Acoust. Soc. Am.* **131**, 92–103 (2012).
- Ross, D. *Mechanics of Underwater Noise*. (Pergamon Press Inc., 1976).
- Clark, C. W. *et al.* Acoustic masking in marine ecosystems: intuitions, analysis, and implication. *MEPS* **395**, 201–222 (2009).
- Rolland, R. M. *et al.* Evidence that ship noise increases stress in right whales. *Proceedings of the Royal Society B: Biological Sciences* **279**, 2363–2368 (2012).
- Nowacek, D. P., Thorne, L. H., Johnston, D. W. & Tyack, P. L. Responses of cetaceans to anthropogenic noise. *Mammal Review* **37**, 81–115 (2007).
- Hatch, L. T., Clark, C. W., Van Parijs, S. M., Frankel, A. S. & Ponirakis, D. W. Quantifying Loss of Acoustic Communication Space for Right Whales in and around a U.S. National Marine Sanctuary. *Conservation Biology* **26**, 983–994 (2012).
- McKenna, M. F., Katz, S. L., Wiggins, S. M., Ross, D. & Hildebrand, J. A. A quieting ocean: Unintended consequence of a fluctuating economy. *J. Acoust. Soc. Am.* **132**, EL169–EL175 (2012).



13. International Maritime Organization (IMO). *International shipping and world trade. Facts and figures*. (2009). <http://www.imo.org> (accessed 03/10/2013).
14. Arveson, P. T. & Vendittis, D. J. Radiated noise characteristics of a modern cargo ship. *J. Acoust. Soc. Am.* **107**, 118–129 (2000).
15. Heitmeyer, R. M., Wales, S. C. & Pflug, L. A. Shipping Noise Predictions: Capabilities and Limitations. *Marine Technology Society Journal* **37** (2003).
16. Wales, S. & Heitmeyer, R. An ensemble source spectra model for merchant ship-radiated noise. *J. Acoust. Soc. Am.* **111**, 1211–1231 (2002).
17. Huyer, A. Coastal upwelling in the California current system. *Progress In Oceanography* **12**, 259–284 (1983).
18. Jensen, F. B., Kuperman, W. A., Porter, M. B. & Schmidt, H. *Computational Ocean Acoustics*. (Springer-Verlag, 1993).
19. Zhou, J., Zhang, X. & Rogers, P. H. Resonant interaction of sound wave with internal solitons in the coastal zone. *J. Acoust. Soc. Am.* **90**, 2042–2054 (1991).
20. McKenna, M. F., Katz, S. L., Condit, C. & Walbridge, S. Response of commercial ships to a voluntary speed reduction measure: Are voluntary strategies adequate for mitigating ship-strike risk? *Coastal Management* **40**, 634–650 (2012).
21. Okumoto, Y., Takeda, Y., Mano, M. & Okada, T. *Design of Ship Hull Structures- A Practical Guide for Engineers*. (Springer-Verlag Berlin Heidelberg: Berlin, Heidelberg, 2009).
22. Port of Long Beach. Port Statistics. (2011). <http://www.polb.com/economics/stats/default.asp> (accessed 10/24/2012).
23. Wiggins, S. & Hildebrand, J. A. High-frequency Acoustic Recording Package (HARP) for broad-band, long-term marine mammal monitoring. *International Symposium on Underwater Technology and International Workshop on Scientific Use of Submarine Cables & Related Technologies* (2007).
24. Tetreault, B. J. Use of Automatic Identification System (AIS) for maritime domain awareness (MDA). *OCEANS Proceedings of MTS/IEEE* **2**, 1590–1594 (2005).
25. Institute for Computational Earth System Sciences (ICEES) project and data description. (2009). <http://www.icess.ucsb.edu/iog/realtime/index.php> (accessed 10/24/2012).
26. IHS Fairplay World Shipping Encyclopedia. (2009). <http://www.ihs.com/products/maritime-information/ships/world-shipping-encyclopedia.aspx> (accessed 10/24/2012).
27. NOAA Station 46053 (LLNR 196) - E. SANTA BARBARA. (2009). http://www.ndbc.noaa.gov/station_page.php?station=46053 (accessed 10/24/2012).
28. Hastie, T. J. & Tibshirani, R. J. *Generalized Additive Models*. (CRC Press, 1990).
29. Wood, S. N. *Generalized additive models: an introduction with R*. (CRC Press, 2006).
30. Akaike, H. *Canonical Correlation Analysis of Time Series and the Use of an Information Criterion*. In *System Identification Advances and Case Studies* (Elsevier: 1976).

Acknowledgments

Funding for this work came from the NOAA-NMFS Office of Science and Technology, Channel Islands National Marine Sanctuary, US Navy and ONR. We thank the captain and crew of the *R/V Shearwater* at the Channel Islands National Marine Sanctuary; C. Garsha, B. Hurley, and T. Christianson for field support; C. Garsha, C. Condit, E. Roth, L. Washburn, B. Emery, C. Johnson, and M. Roche for assistance with the AIS system; J. Watson, J. Barlow, B. Hodgkiss, and J. Leichter for helpful comments on the content and writing of the manuscript. This manuscript is in partial fulfillment of the lead author's Ph.D. thesis.

Author contributions

M.F.M. performed the analysis, wrote the manuscript text and prepared figures. J.A.H. and S.M.W. developed the acoustic instrumentation. M.F.M. designed the AIS data collection system. M.F.M., S.M.W., J.A.H. reviewed and edited the manuscript.

Additional information

Supplementary information accompanies this paper at <http://www.nature.com/scientificreports>

Competing financial interests: The authors declare no competing financial interests.

License: This work is licensed under a Creative Commons Attribution-NonCommercial-NoDerivs 3.0 Unported License. To view a copy of this license, visit <http://creativecommons.org/licenses/by-nc-nd/3.0/>

How to cite this article: McKenna, M.F., Wiggins, S.M. & Hildebrand, J.A. Relationship between container ship underwater noise levels and ship design, operational and oceanographic conditions. *Sci. Rep.* **3**, 1760; DOI:10.1038/srep01760 (2013).